JOC*Article*

Hydrogen-Bonded Networks in Organic Conductors: Crystal Structures and Electronic Properties of Charge-Transfer Salts of Tetracyanoquinodimethane with 4,4′-Biimidazolium Having Multiprotonated States

Yasushi Morita,*,†,‡ Tsuyoshi Murata,† Kozo Fukui,‡ Satoru Yamada,† Kazunobu Sato,§ Daisuke Shiomi,§ Takeji Takui,§ Hiroshi Kitagawa,∥ Hideki Yamochi,⊥ Gunzi Saito,⊥ and Kazuhiro Nakasuji*,†

Department of Chemistry, Graduate School of Science, Osaka University, Toyonaka, Osaka 560-0043, Japan, Departments of Chemistry and Materials Science, Graduate School of Science, Osaka City University, Sumiyoshi-ku, Osaka 558-8585, Japan, Department of Chemistry, Graduate School of Science, Kyusyu University, Fukuoka, Fukuoka 812-8581, Japan, Division of Chemistry, Graduate School of Science, and Research Center for Low Temperature and Materials Science, Kyoto University, Sakyo-ku, Kyoto 606-8502, Japan, and PRESTO, JST, Kawaguchi, Saitama 332-0012, Japan

morita@chem.sci.osaka-u.ac.jp

Received December 21, 2004

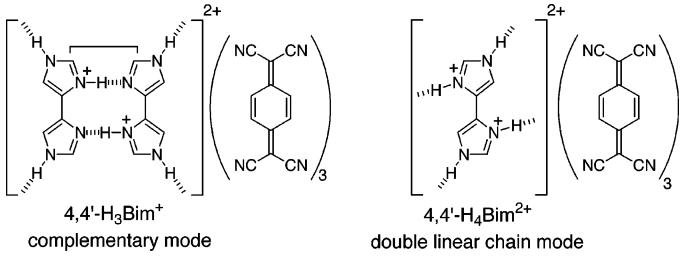

Novel hydrogen-bonded charge-transfer salts of TCNQ with mono- and diprotonated 4,4'-biimidazolium were synthesized in order to demonstrate the high potential of the 4,4'-biimidazole system in a molecular conductor from the viewpoint of crystal engineering and electronic modulation. Crystal structure analyses of neutral 4,4'-biimidazole and TCNQ salts revealed the formation of two types of hydrogen-bonding modes of the 4,4'-biimidazole moiety depending on the protonated states. Neutral 4,4'-biimidazole possessed a linear chain mode of hydrogen-bonding to construct two-dimensional network. In the TCNQ salt of monoprotonated 4,4'-biimidazolium, the 4,4'-biimidazole moiety formed a dimer by a complementary mode of hydrogen-bonding. In contrast, the salt of diprotonated 4,4'-biimidazolium showed a double linear chain mode of hydrogen-bonding to construct a three-dimensional network. The formation of two types of hydrogen-bonding modes made the difference in the stacking patterns of TCNQ columns and in their transport properties. The TCNQ salt of diprotonated 4,4'-biimidazolium exhibited high electrical conductivity ($\sigma_{rt} = 1.1 \times 10^{-1}$ S cm^{-1}).

Introduction

Hydrogen-bonding (H-bonding) interaction, serving as a vital role in the formation of biological structures such as DNA-double helix, attracts much attention from the viewpoint of molecular recognition, crystal engineering, and supramolecular chemistry.[1] Introduction of H-bonding interaction into charge-transfer (CT) complexes and salts is recognized as an important methodology in the creation of new organic conductors by controlling the relative molecular aggregation with increasing dimensionality of the network structure.[2] Recent successful preparations of metallic H-bonded CT salts of tetrathiafulvalene (TTF) derivatives furnished by Batail and coworkers are typical examples achieved by an effective

* To whom correspondence should be addressed. Tel: +81-6-6850-5393. Fax: +81-6-6850-5395.
† Osaka University.
‡ PREST, JST.
§ Osaka City University.
∥ Kyusyu University.
⊥ Kyoto University.

(1) For a recent overview of H-bonding, see: *The Weak Hydrogen Bond*; Desiraju, G. R., Steiner, T., Eds.; Oxford University Press: New York, 1999; Chapter 1.

10.1021/jo047768c CCC: $30.25 © 2005 American Chemical Society
Published on Web 03/03/2005

crystal engineering.[3] In addition to these potential structural aspects, we have recently demonstrated two types of the new function of H-bonding interactions to modulate electronic structures of CT complexes.[4,5] One is to control ionicities by regulating the component ratio of donor and acceptor molecules by specific H-bondings, as exemplified by a chloranil complex of TTF−imidazole.[4] The other is to enhance an electron-donating ability of donor molecule by H-bonding formation through directly introduced substituents into the π-system of donor molecule, as demonstrated by tetracyanoquinodimethane (TCNQ) complex of diaminodibenzo-TTF.[5] From these viewpoints, the construction of CT complexes and salts having well-defined multidimensional H-bonding networks is an important issue in the development of organic conductors.

What kinds of molecules one may use as components of H-bonded CT complexes and salts is of primary importance. As for the anionic part, TCNQ radical anions have played a central role from an early stage of the research for molecular conductors in the 1960s.[6] Despite a variety of TCNQ salts with ammonium-type cations as H-bonded CT salts being examined, very few works have been reported to address the salts showing high conductivities with multidimensional H-bonded networks between TCNQ and cationic moieties.[6,7] Therefore, further development is required to design more suitable counterions with sufficient H-bonding ability having robust directionality and to build up highly ordered multidimensional network based on H-bonded TCNQ salts.

2,2'-Biimidazole (2,2'-H_2Bim) system, well-known as a bidentate ligand for transition metals, possesses multi proton-accepting and -donating sites and is expected to construct diverse H-bonded structures depending on its protonated states. Actually, 2,2'-H_2Bim has been utilized as a building block of assembled metal complexes[8] and supramolecular assemblies[9] with characteristic H-bonding structures in each protonated state. Furthermore, Akutagawa and co-workers demonstrated the H-bonded

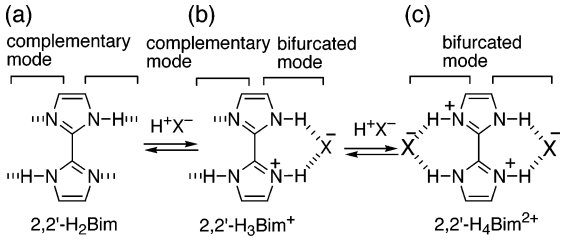

FIGURE 1. Scheme of the H-bonding modes of 2,2'-H_2Bim depending on the protonated states: (a) neutral, (b) monoprotonated, and (c) diprotonated.

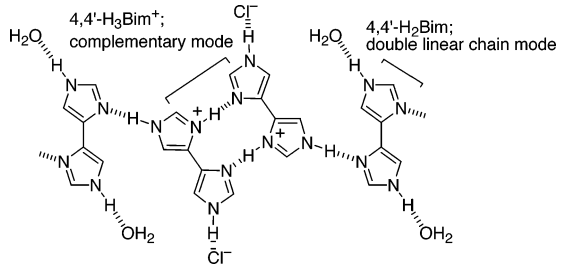

FIGURE 2. Schematic representation of the H-bonded zigzag-ribbon structure in the crystal structure of (4,4'-H_2Bim)(4,4'-$H_3Bim^+)_2Cl^-_2(H_2O)_2$ (**1**).

structures and electronic properties of 2,2'-H_2Bim and 2,2'-bibenzimidazole (2,2'-H_2BBim) systems in their TCNQ salts.[10,11] The H-bonding modes of 2,2'-H_2Bim depending on the protonated states are schematically illustrated in Figure 1: (a) complementary mode of H-bondings in neutral state, (b) complementary mode having bifurcated mode in monoprotonated state, (c) double bifurcated modes to bridge two anions in diprotonated state (Figure 1).[9,10]

To explore further H-bonded supramolecular assemblies with intriguing functionalities based on the imidazole-ring system, we have recently synthesized novel 4,4'-biimidazole (4,4'-H_2Bim) and oligo(imidazole)s.[12] In the hydrochloric acid salt of 4,4'-H_2Bim containing a neutral component, (4,4'-H_2Bim)(4,4'-$H_3Bim^+)_2Cl^-_2(H_2O)_2$ (**1**),[12a] and its metal complexes,[12b] the 4,4'-H_2Bim system exhibited directional H-bonded structures different from those of the 2,2'-H_2Bim system (Figure 2, vide infra). These unique H-bonding features and multiprotonated states in the 4,4'-H_2Bim system show that this system is a good candidate for the H-bonded counterion in the TCNQ radical anion salts in the investigation for molec-

(2) (a) Bryce, M. R. *J. Mater. Chem.* **1995**, *5*, 1481−1495. (b) Batail, P.; Boubekeur, K.; Fourmigué, M.; Gabriel, J.-C. P. *Chem. Mater.* **1998**, *10*, 3005−3015. (c) Fourmigué, M.; Batail, P. *Chem. Rev.* **2004**, *104*, 5379−5418. (d) Morita, Y.; Maki, S.; Ohmoto, M.; Kitagawa, H.; Okubo, T.; Mitani, T.; Nakasuji, K. *Org. Lett.* **2002**, *4*, 2185−2188.

(3) (a) Heuzé, K.; Fourmigué, M.; Batail, P.; Canadell, E.; Auban-Senzier, P. *Chem. Eur. J.* **1999**, *5*, 2971−2976. (b) Heuzé, K.; Mézière, C.; Fourmigué, M.; Batail, P.; Coulon, C.; Canadell, E.; Auban-Senzier, P.; Jérome, D. *Chem. Mater.* **2000**, *12*, 1898−1904.

(4) Murata, T.; Morita, Y.; Fukui, K.; Sato, K.; Shiomi, D.; Takui, T.; Maesato, M.; Yamochi, H.; Saito, G.; Nakasuji, K. *Angew. Chem., Int. Ed.* **2004**, *43*, 6343−6346.

(5) Morita, Y.; Miyazaki, E.; Fukui, K.; Maki, S.; Nakasuji, K. To be submitted for publication.

(6) (a) Melby, L. R.; Harder, R. J.; Hertler, W. R.; Mahler, W.; Benson, R. E.; Mochel, W. E. *J. Am. Chem. Soc.* **1962**, *84*, 3374−3387. (b) Torrance, J. B. *Acc. Chem. Res.* **1979**, *12*, 79−86.

(7) (a) Kobayashi, H.; Ohashi, Y.; Marumo, F.; Saito, Y. *Acta Crystallogr., Sect. B* **1970**, *26*, 459−467. (b) Kobayashi, H.; Marumo, F.; Saito, Y. *Acta Crystallogr., Sect. B* **1971**, *27*, 373−378. (c) Kobayashi, H. *Bull. Chem. Soc. Jpn.* **1974**, *47*, 1346−1352. (d) Truong, K. D.; Pépin, C.; Bandrauk, A. D.; Drouin, M.; Michel, A.; Banville, M. *Can. J. Chem.* **1991**, *69*, 1804−1811. (e) Usov, O. A.; Burshtein, I. A.; Kartenko, N. F.; Rozhdestvenskaya, I. V.; Vlasova, R. M.; Semkin, V. N.; Abashev, G. G.; Russkikh, V. S. *Acta Crystallogr., Sect. C* **1991**, *47*, 1851−1854. (f) Inabe, T.; Okaniwa, K.; Ogata, H.; Okamoto, H.; Mitani, T.; Maruyama, Y. *Acta Chim. Hung.* **1993**, *130,* 537−554.

(8) (a) Tadokoro, M.; Isobe, K.; Uekusa, H.; Ohashi, Y.; Toyoda, J.; Tashiro, K.; Nakasuji, K. *Angew. Chem., Int. Ed.* **1999**, *38*, 95−98. (b) Tadokoro, M.; Nakasuji, K. *Coord. Chem. Rev.* **2000**, *198*, 205−218. (c) Tadokoro, M.; Kanno, H.; Kitajima, T.; Umemoto, H.-S.; Nakanishi, N.; Isobe, K.; Nakasuji, K. *Proc. Natl. Acad. Sci. U.S.A.* **2002**, *99*, 4950−4955.

(9) (a) Cromer, D. T.; Ryan, R. R.; Storm, C. B. *Acta Crystallogr., Sect. C* **1987**, *43*, 1435−1437. (b) Bélanger, S.; Beauchamp, A. L. *Acta Crystallogr., Sect. C* **1996**, *52*, 2588−2590. (c) Allen, W. E.; Fowler, C. J.; Lynch, V. M.; Sessler, J. L. *Chem. Eur. J.* **2001**, *7*, 721−729. (d) Ramírez, K.; Reyes, J. A.; Briceño, A.; Atencio, R. *CrystEngComm* **2002**, *4*, 218−212.

(10) Akutagawa, T.; Saito, G.; Kusunoki, M.; Sakaguchi, K. *Bull. Chem. Soc. Jpn.* **1996**, *69*, 2487−2511.

(11) (a) Akutagawa, T.; Hasegawa, T.; Nakamura, T.; Inabe, T.; Saito, G. *Chem. Eur. J.* **2002**, *8*, 4402−4411. (b) Akutagawa, T.; Hasegawa, T.; Nakamura, T.; Saito, G. *CrystEngComm* **2003**, *5*, 54−57.

(12) (a) Morita, Y.; Murata, T.; Yamada, S.; Tadokoro, M.; Ichimura, A.; Nakasuji, K. *J. Chem. Soc., Perkin Trans. 1* **2002**, 2598−2600. (b) Morita, Y.; Murata, T.; Fukui, K.; Tadokoro, M.; Sato, K.; Shiomi, D.; Takui, T.; Nakasuji, K. *Chem. Lett.* **2004**, *33*, 188−189. (c) Murata, T.; Morita, Y.; Nishimura, Y.; Nakasuji, K. *Polyhedron*, in press. See also, (d) Zhang, W.; Landee, C. P.; Willett, R. D.; Turnbull, M. M. *Tetrahedron* **2003**, *59*, 6027−6034.

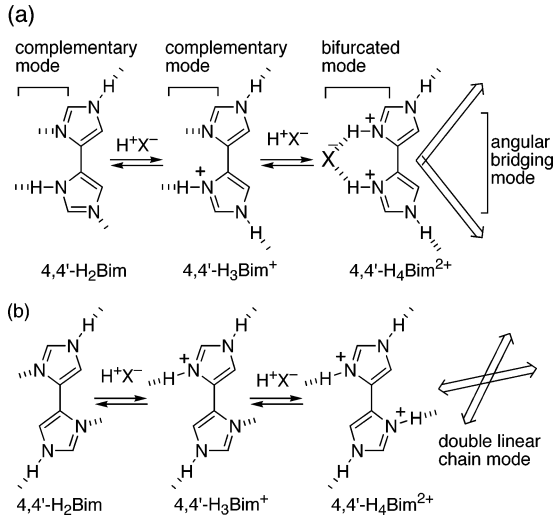

FIGURE 3. Scheme of the H-bonding modes depending on the protonated states and conformations of 4,4'-H_2Bim in (a) *cis*-conformation and (b) *trans*-conformation.

ular assemblies having interesting conducting properties. Herein we report the first disclosure of the crystal structures of neutral 4,4'-H_2Bim and its TCNQ salts, monoprotonated salt (4,4'-$H_3Bim^+)_2(TCNQ)_3$ (**2**) and diprotonated salt (4,4'-H_4Bim^{2+})$(TCNQ)_3(H_2O)_2$ (**3**). In these TCNQ salts, we emphasize that the differences of the protonated states and H-bonding modes of 4,4'-H_2Bim moieties control the electronic states of TCNQ moieties, the stacking patterns in TCNQ columns, and the transport properties of the salts.

Results and Discussion

Preparation. Single crystals of neutral 4,4'-H_2Bim were obtained by the vapor diffusion method using ethyl acetate−EtOH. The hydroiodic acid salts, (4,4'-H_3Bim^+)-I^- and (4,4'-H_4Bim^{2+})$2I^-$, were prepared by mixing of 4,4'-H_2Bim and one and three equivalent of hydrogen iodide in hot EtOH, respectively. Diffusion of EtOH solution of (4,4'-H_3Bim^+)I^- and $Li^+TCNQ^{\bullet-}$ gave single crystals of salt **2** suitable for X-ray crystal analysis. The TCNQ salt of 4,4'-H_4Bim^{2+}, **3**, was prepared by the metathesis method between iodide salt of diprotonated 4,4'-biimidazolium and $Li^+TCNQ^{\bullet-}$ in MeOH. Single crystals of **3** were obtained by aerial evaporation of its acetone-H_2O solution.

H-Bonding Modes of 4,4'-H_2Bim Depending on the Protonated States and Conformation. 4,4'-H_2Bim system is expected to form a variety of H-bonding modes depending on its protonated states and conformations. In the crystal structure of the salt **1**, H-bonding modes of neutral 4,4'-H_2Bim and monoprotonated 4,4'-H_3Bim^+ were double linear chain mode with *trans*-conformation and complementary dimer mode with *cis*-conformation to construct zigzag-ribbon structure (Figure 2). From this result, we have summarized the possible H-bonding modes of 4,4'-H_2Bim system in each protonated states and conformations (Figure 3). In the *cis*-conformation, 4,4'-H_2Bim system forms angular bridging and complementary modes of H-bondings (Figure 3a). In sharp contrast, in *trans*-conformation, it forms a double linear chain mode of H-bondings (Figure 3b). These H-bonding

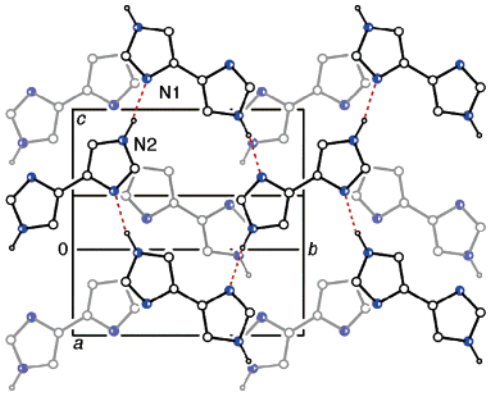

FIGURE 4. Crystal structure of neutral 4,4'-H_2Bim, showing the two-dimensional H-bonded sheet structure. Dotted lines show the N(1)−H···N(2) H-bondings (2.84 Å). The light colored molecular network belongs in the next sheet of the forefront network. For details, see the Supporting Information.

modes in 4,4'-H_2Bim system are preferable to construct multidimensional H-bonded networks compared to those in 2,2'-H_2Bim system. These features of H-bonding directionalities inherent in two H_2Bim isomers can control the H-bonded networks in the solid state, and affect the molecular packing and physical properties in their CT salts.

Crystal Structures. Neutral 4,4'-H_2Bim possesses a planar molecular structure and the *trans*-conformation with an inversion center on central C−C bond. The neighboring 4,4'-H_2Bim molecules are connected by N(1)−H···N(2) H-bondings with the dihedral angle of ca. 33° to form two-dimensional sheet structure (Figure 4). This sheet structure stacks with slipping by nearly one molecule and no $\pi-\pi$ interactions were found. The *trans*-conformation and linear chain mode of H-bondings in this structure show a resemblance to those of neutral 4,4'-H_2Bim moiety in the structure of salt **1**.[12a]

The TCNQ salt of monoprotonated 4,4'-H_3Bim^+, (4,4'-$H_3Bim^+)_2(TCNQ)_3$ (**2**), is composed of 4,4'-H_3Bim^+ and two kinds of crystallographically independent TCNQ molecules (TCNQ-A and TCNQ-B, A/B = 2:1) (Figure 5). The ionicities of TCNQ-A and -B are deduced as 0.92 and 0.28, respectively, from bond lengths of TCNQs, $c/(b + d)$ (Table 1).[13] TCNQ molecules stack to form a columnar structure in the manner of TCNQ-A-A-B along the *b*-axis. The stacking modes in the columnar structure are a nearly eclipsed mode for TCNQ-A and -A and a ring-over-bond mode for TCNQ-A and -B with the face-to-face distances of 3.24 and 3.23 Å, respectively (Figure 5a,b). The 4,4'-H_3Bim^+ moiety adopts the *cis*-conformation and forms a dimer, $(4,4'\text{-}H_3Bim^+)_2$, by the complementary mode of H-bonding. Four N−H groups on the dimer connect the TCNQ columns by the angular bridging mode of H-bondings through TCNQ-A molecules (Figure 5c). These H-bonding interactions, N(1)−H···N(6)≡C and N(3)−H···N(7)≡C, are directed along the [101] in the crystal.

The TCNQ salt of diprotonated 4,4'-H_4Bim^{2+}, (4,4'-H_4-Bim^{2+})$(TCNQ)_3(H_2O)_2$ (**3**), contains 4,4'-H_4Bim^{2+} dication, two kinds of crystallographically independent TCNQ

(13) (a) Flandrois, P. S.; Chasseau, D. *Acta Crystallogr., Sect. B* **1977**, *33*, 2744−2750. (b) Kistenmacher, T. J.; Emge, T. J.; Bloch, A. N.; Cowan, D. O. *Acta Crystallogr., Sect. B* **1982**, *38*, 1193−1199.

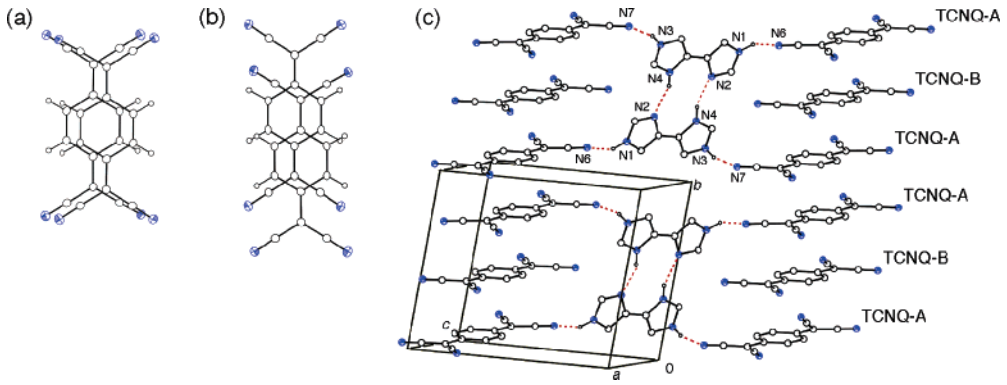

FIGURE 5. Crystal structure of $(4,4'\text{-}H_3Bim^+)_2(TCNQ)_3$ (**2**). Overlaps in TCNQ column: (a) nearly eclipsed modes of two TCNQ-A, (b) ring-over-mode of TCNQ-A and -B. (c) Crystal packing showing the one-dimensional column of TCNQ molecules, square-shaped H-bonded dimer of $4,4'\text{-}H_3Bim^+$ and H-bonded network connecting the columnar structures. H-bonding distances (D···A in Å): N(2)···N(4), 2.80; N(1)···N(6), 2.88; and N(3)···N(7), 2.92.

TABLE 1. Intramolecular C−C Bond Lengths of TCNQ Moiety in Salts 2 and 3, Neutral $TCNQ^0$, and Completely Ionic $TCNQ^{\bullet-}$

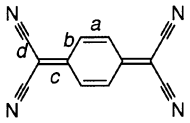

	a/Å	*b*/Å	*c*/Å	*d*/Å
2, TCNQ-A	1.367	1.425	1.416	1.420
2, TCNQ-B	1.353	1.443	1.387	1.431
3, TCNQ-A	1.352	1.425	1.405	1.419
3, TCNQ-B	1.339	1.437	1.374	1.427
$TCNQ^0$ [13a]	1.346	1.448	1.374	1.441
$TCNQ^{\bullet-}$ [13b]	1.373	1.426	1.420	1.416

molecules (TCNQ-A and TCNQ-B, A/B = 2:1), and water molecules (Figure 6). The molecular structure of $4,4'\text{-}H_4Bim^{2+}$ dication possesses the *trans*-conformation and an inversion center on the central C−C bond. The intramolecular C−C bond lengths of TCNQ molecules gave the ionicities of TCNQ-A and -B as 0.75 and 0.17, respectively (Table 1).[13] The TCNQ molecules form one-dimensional π-stacking columns in the manner of TCNQ-A-A-B with face-to-face distances of 3.03 Å for TCNQ-A and -A, and 3.24 Å for TCNQ-A and -B. Contrary to the stacking mode in the TCNQ column of salt **2**, all TCNQ molecules stack with the ring-over-bond mode (Figure 6a,b). The $4,4'\text{-}H_4Bim^{2+}$ molecule is located between the TCNQ layers in the *ab* plane and the longitudinal axis of the dication is parallel to the acceptor columns. The H-bondings of the dication, N(2)−H···N(6)≡C and N(1)−H···O(1), adopt the double linear chain mode. The N(2)−H···N(6)≡C H-bonding connects the TCNQ columns along the [-101] direction, and two N(1)−H groups connect six TCNQ-A molecules through H-bonding interactions with water molecules (Figure 6c). These H-bondings build up the three-dimensional H-bonded network and highly contribute to the formation of this molecular packing.

Spectral and Physical Properties. The protonated states of $4,4'\text{-}H_2Bim$ moieties in salt **2** and **3** were evaluated by comparing the frequency of in-plane N−H bending mode (δ_{NH}) in the IR spectra with those of $4,4'\text{-}H_2Bim$, $4,4'\text{-}H_3Bim^+$ and $4,4'\text{-}H_4Bim^{2+}$ salt (Figure 7);[14] δ_{NH} was observed at 1533 cm^{-1} for $4,4'\text{-}H_2Bim$, 1580 and 1554 cm^{-1} for $4,4'\text{-}H_3Bim^+$, and 1568 cm^{-1} for $4,4'\text{-}H_4Bim^{2+}$. The salt **2** exhibits the absorption band at 1563 cm^{-1} assignable to the δ_{NH} mode of $4,4'\text{-}H_3Bim^+$. The other band of $4,4'\text{-}H_3Bim^+$ is overlapped with B_{1u} modes of C=C stretching of $TCNQ^{\bullet-}$ molecule (1581 cm^{-1}).[15] The bands at 1531 and 1505 cm^{-1} were assigned to B_{1u} mode of $TCNQ^0$ and B_{2u} mode of $TCNQ^{\bullet-}$, respectively.[15] The salt **3** shows the δ_{NH} band at 1575 cm^{-1} which is close to that of $4,4'\text{-}H_4Bim^{2+}$ salt. Additionally, the disappearance of δ_{NH} modes of $4,4'\text{-}H_2Bim$ and $4,4'\text{-}H_3Bim^+$ indicates the absence of these species in **3**. Thus, the protonated state of **3** was determined to be dication. The shoulder band (1584 cm^{-1}) overlapped with the δ_{NH} mode of $4,4'\text{-}H_4Bim^{2+}$ and single band (1505 cm^{-1}) were assigned to be B_{1u} and B_{2u} modes of C=C stretching of $TCNQ^{\bullet-}$ molecules, respectively.[15]

The protonated states and stoichiometries of biimidazolium and TCNQ moieties in **2** and **3** gave the calculated average ionicity of TCNQ of 0.67 which is comparable to those estimated from the B_{1u} mode of the nitrile stretching frequency of TCNQ moiety, 0.75 (2194 cm^{-1}) for **2** and 0.70 (2196 cm^{-1}) for **3**.[16] The salt **3** shows a broad absorption band at around 3200 cm^{-1}, which is assigned to be the intracolumnar CT transition from $TCNQ^{\bullet-}$ to $TCNQ^0$,[17] while the salt **2** shows the CT band at higher energy region, 4600 cm^{-1} (Figure 8).

The measurements of electrical conductivity for compressed pellets of salt **2** and **3** show room-temperature conductivities (σ_{rt}) of 1.5×10^{-4} and 1.1×10^{-1} S cm^{-1} with activation energy 265 and 113 meV, respectively. The σ_{rt} value of TCNQ salt of $4,4'\text{-}H_4Bim^{2+}$ is five to six orders higher than those of TCNQ salts of $2,2'\text{-}H_2Bim$.[18] The magnetic susceptibility of **3** was measured for polycrystalline sample in the range of 1.9−298 K (Figure 9). The paramagnetic susceptibility, χ_p, was fully described by singlet−triplet model. The triplet activation

(14) Akutagawa et al. also investigated the protonated state of $2,2'\text{-}H_2Bim$ and $2,2'\text{-}H_2BBim$ in the CT salts using δ_{NH} values.[10,11]

(15) (*a*) Fritchie, C. J.; Arthur, P. *Acta Crystallogr., Sect. B* **1966**, *21*, 139−145. (*b*) Cummings, K. D.; Tanner, D. B.; Miller, J. S. *Phys. Rev.* **1981**, *B24*, 4142−4154.

(16) Chappell, J. S.; Bloch, A. N.; Bryden, W. A.; Maxfield, M.; Poehler, T. O.; Cowan, D. O. *J. Am. Chem. Soc.* **1981**, *103*, 2442−2443.

(17) Torrance, J. B.; Scott, B. A.; Kaufman, F. B. *Solid State Commun.* **1975**, *17*, 1369−1373.

(18) σ_{rt} values of TCNQ salts of 2, $2'\text{-}H_2Bim$; 5.9×10^{-8} S cm^{-1} for $(2,2'\text{-}H_3Bim^+)(TCNQ)$, 8.3×10^{-7} S cm^{-1} for $(2,2'\text{-}H_3Bim^+)_2(TCNQ)_3$, 1.6×10^{-7} S cm^{-1} for $(2,2'\text{-}H_4Bim^{2+})(TCNQ)_2$.[10]

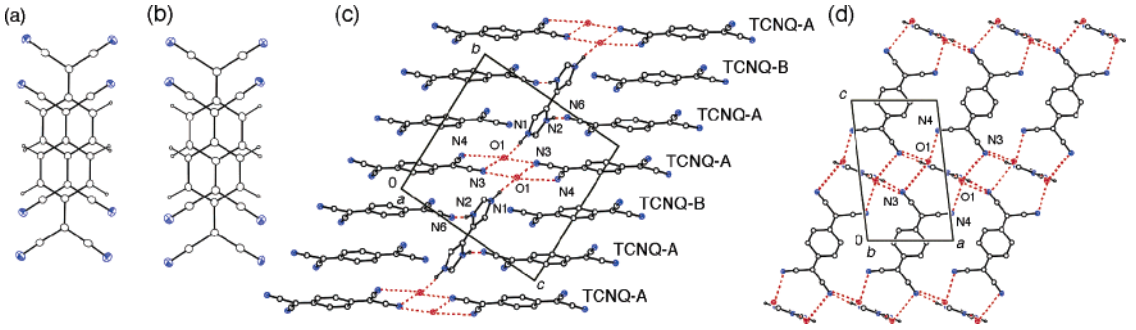

FIGURE 6. Crystal structure of (4,4'-H_4Bim^{2+})$(TCNQ)_3(H_2O)_2$ (**3**). Overlap modes of (a) two TCNQ-A, and (b) TCNQ-A and -B in the TCNQ column. Crystal packing showing the one-dimensional column of TCNQ molecules with H-bonded network viewed along (c) the *a*-axis, (d) the *b*-axis. H-bonding distances (D···A in Å): N(1)···O(1), 2.69; N(2)···N(6), 2.85; N(3)···O(1), 2.95 and 3.14; N(4)···(O1), 3.01.

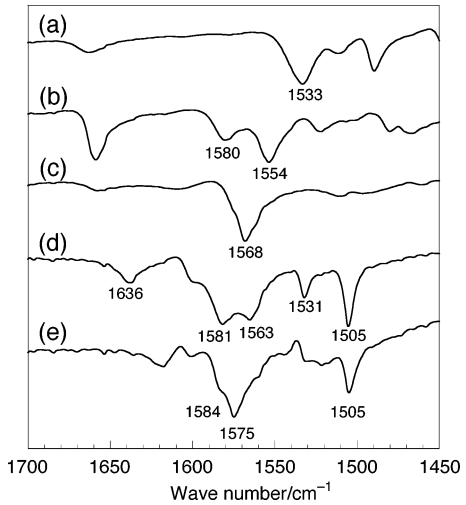

FIGURE 7. IR spectra of (a) 4,4'-H_2Bim, (b) (4,4'-H_3Bim^+)I^-, (c) (4,4'-H_4Bim^{2+})$2I^-$, (d) (4,4'-H_3Bim^+)$_2(TCNQ)_3$ (**2**), and (e) (4,4'-H_4Bim^{2+})$(TCNQ)_3(H_2O)_2$ (**3**) in the frequency range 1450−1700 cm^{-1} measured by KBr pellet.

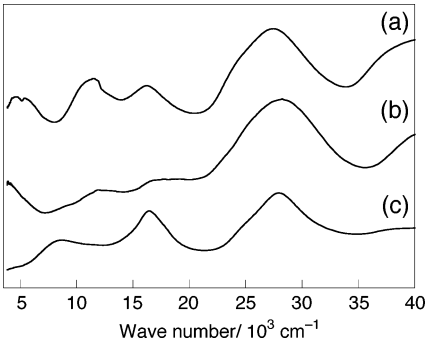

FIGURE 8. Electronic spectra of (a) (4,4'-H_3Bim^+)$_2(TCNQ)_3$ (**2**), (b) (4,4'-H_4Bim^{2+})$(TCNQ)_3(H_2O)_2$ (**3**), and (c) $K^+TCNQu^{\bullet-}$ measured by KBr pellet.

energy was determined by Bleany−Bowers equation[19] to be 108 meV (−1248 K), being in good agreement with the value from the electrical conductivity measurement. This coincidence suggests that the electrical conduction is caused by intracolumnar transfer of exciton that is induced by thermal activation of TCNQ-A dimer. The

(19) Bleaney, B.; Bowers, K. D. *Proc. R. Soc. London Ser. A* **1952**, *214*, 451−465.

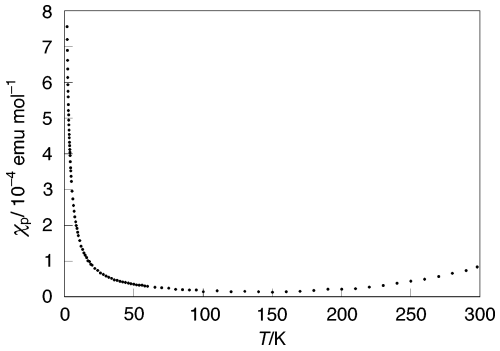

FIGURE 9. Temperature dependence of paramagnetic susceptibility (χ_p) for the polycrystalline sample of (4,4'-H_4Bim^{2+})-$(TCNQ)_3(H_2O)_2$ (**3**). The diamagnetic susceptibility was estimated to be -4.04×10^{-4} emu mol^{-1} and subtracted. The χ_p values are described by the Bleaney−Bowers equation[19] (see text), assuming 0.47% of doublet impurity radicals.

relatively high electrical conductivity in **3** may be associated with its columnar structure of TCNQ; the more regular overlapping mode of TCNQ column in **3** (Figure 6a,b) seems to make electrical conduction favorable. This also enhances the delocalization of negative charge on TCNQ moieties and reduces the electric repulsion. The marked difference in electrical conductivities between two salts, **2** and **3**, results from the formation of two types of H-bonding modes with robust directionality and multidimensional H-bonded network constructed by 4,4'-H_3-Bim^+ and 4,4'-H_4Bim^{2+}. Therefore, in these H-bonded CT salts, crystal structures and electrical properties are controlled by the subtle balance in the relative molecular aggregation and the geometry of *cis*−*trans* conformation inherent in the 4,4'-H_2Bim systems (Figure 3b,c).

Conclusion

The neutral state of 4,4'-H_2Bim and two kinds of CT salts of TCNQ with mono- and diprotonated 4,4'-biimidazolium were investigated for the first time. In the crystal structure, 4,4'-H_2Bim system formed two types of H-bonding mode depending on the protonated states; double linear chain mode of 4,4'-H_2Bim and 4,4'-H_4Bim^{2+} and complementary mode of 4,4'-H_3Bim^+. The difference in the H-bonding modes in the TCNQ salts **2** and **3** affects the stacking pattern of TCNQ moieties to make the difference in their transport properties by 3 orders of magnitude. Thus, multidimensional H-bondings shown

in TCNQ salts of 4,4'-H_3Bim^+ and 4,4'-H_4Bim^{2+} reveal the high potential of 4,4'-H_2Bim system as an effective intermolecular interaction for the crystal engineering and electronic modulation in the development of molecular conductors. Furthermore, the classification of the H-bonding styles of 4,4'-H_2Bim system depending on the protonated states and conformation gives important information in the design for supramolecular assemblies. Developing new CT salts and complexes with highly ordered H-bonding interaction based on imidazole-ring systems can enable chemists to evolve molecular design for the construction of new organic conductors with intriguing molecular functionalities, which serves for the realization of cooperative proton−electron system.[20]

Experimental Section[21]

4,4'-Biimidazolium Monoiodide [(4,4'-H_3Bim^+)I^-]. 4,4'-H_2Bim (268 mg, 2.00 mmol) was placed in a 50-mL round-bottomed flask and dissolved with EtOH (25 mL). HI (55% aqueous solution, 0.30 mL, 2.19 mmol) was added to this mixture at room temperature. The reaction mixture was stirred at room temperature for 0.5 h, and then left standing at −30 °C for 18 h. The resulting powder was collected by filtration and washed with ethyl acetate (10 mL) to give the monoprotonated salt as a white powder (218 mg, 42%): mp 259−260 °C dec; ^{1}H NMR (270 MHz, DMSO-d_6, 80 °C) δ 7.67 (s, 2H), 8.39 (s, 2H); IR (KBr) 3300−2200, 1659, 1580, 1554 cm^{-1}. Anal. Calcd for $C_6H_7N_4I$: C, 27.50; H, 2.69; N, 21.38. Found: C, 27.63; H, 2.61; N, 21.38.

4,4'-Biimidazolium Diiodide [(4,4'-H_4Bim^{2+})2I^-]. 4,4'-H_2-Bim (151 mg, 1.13 mmol) was placed in a 100-mL round-bottomed flask and dissolved with EtOH (18 mL). HI (55% aqueous solution, 0.49 mL, 3.37 mmol) was added to this mixture at room temperature. The reaction mixture was refluxed for 3 h, and then left standing at 0 °C for 12 h. The resulting powder was collected by filtration and washed with Et_2O (10 mL) to give the diprotonated salt as a white powder (401 mg, 91%): mp 256−258 °C; ^{1}H NMR (270 MHz, DMSO-d_6, 80 °C) δ 7.84 (s, 2H), 8.78 (s, 2H); IR (KBr) 3300−2400, 1568 cm^{-1}. Anal. Calcd for $C_6H_8N_4I_2$: C, 18.48; H, 2.07; N, 14.37. Found: C, 18.53; H, 1.90; N, 14.35.

TCNQ Salt of Monoprotonated 4,4'-Biimidazolium [(4,4'-H_3Bim^+)$_2$(TCNQ)$_3$] (2). The (4,4'-H_3Bim^+)I^- (52.4 mg, 0.20 mmol) in MeOH (15 mL) was placed in a 50-mL round-bottomed flask. $Li^+TCNQ^{\bullet-}$ (42.2 mg, 0.20 mmol) in MeOH (8 mL) was added slowly to the mixture. After being stirred at room temperature for 30 min, the mixture was left standing at room temperature for 2 h. The resulting solid was collected by filtration and washed with Et_2O (5 mL) to give the CT salt as a black crystals (18.2 mg, 21%): mp 163−165 °C dec; IR (KBr) 2216, 2194, 2184, 2161, 1636, 1581, 1563, 1531, 1505 cm^{-1}; UV (KBr) 2200, 870, 616, 364 nm. Anal. Calcd for $(C_6H_7N_4)_2(C_{12}H_4N_4)_3$: C, 65.30; H, 2.97; N, 31.73. Found: C, 65.46; H, 2.88; N, 31.51.

TCNQ Salt of Diprotonated 4,4'-Biimidazolium [(4,4'-H_4Bim^{2+})(TCNQ)$_3$(H_2O)$_2$] (3). (4,4'-H_4Bim^{2+})2I^- (50 mg, 0.13 mmol) in MeOH (10 mL) was placed in a 50-mL round-bottomed flask. $Li^+TCNQ^{\bullet-}$ (55 mg, 0.26 mmol) in MeOH (10 mL) was added slowly to the mixture. After being stirred at room temperature for 30 min, the mixture was left standing at 0 °C for 12 h. The resulting powder was collected by filtration and washed with MeOH (2 mL) cooled to 0 °C and Et_2O (5 mL) to give the CT salt as a black powder (39 mg, 57%): mp 154−155 °C dec; IR (KBr) 2196, 2180, 2166, 1575, 1505 cm^{-1}; UV (KBr) 812, 608, 364 nm. Anal. Calcd for $(C_6H_8N_4)(C_{12}H_4N_4)_3(H_2O)_2$: C, 64.28; H, 3.08; N, 28.56. Found: C, 64.58; H, 2.93; N, 28.52.

Acknowledgment. This work was partially supported by a Grant-in-Aid for Scientific Research (No. 16350074) from the Ministry of Education, Culture, Sports, Science, and Technology, Japan, by PRESTO-JST, by a grant of The Asahi Glass Foundation, and by 21COE program "Creation of Integrated EcoChemistry of Osaka University".

Supporting Information Available: General experimental information, IR spectra, electrical conductivity, a list of X-ray crystallographic data for neutral 4,4'-H_2Bim and the TCNQ salts **2**, **3**, and X-ray data in CIF format. This material is available free of charge via the Internet at http://pubs.acs.org.

JO047768C

(20) Nakasuji, K.; Sugiura, K.; Kitagawa, T.; Toyoda, J.; Okamoto, H.; Okaniwa, K.; Mitani, T.; Yamamoto, H.; Murata, I.; Kawamoto, A.; Tanaka, J. *J. Am. Chem. Soc.* **1991**, *113*, 1862−1864.

(21) See the Supporting Information for general experimental methods.